Identification of cofilin and LIM-domain-containing protein kinase 1 as novel interaction partners of 14-3-3ζ

Jörg BIRKENFELD, Heinrich BETZ[1] and Dagmar ROTH

Department of Neurochemistry, Max-Planck-Institute for Brain Research, Deutschordenstrasse 46, 60528 Frankfurt, Germany

Proteins of the 14-3-3 family have been implicated in various physiological processes, and are thought to function as adaptors in various signal transduction pathways. In addition, 14-3-3 proteins may contribute to the reorganization of the actin cytoskeleton by interacting with as yet unidentified actin-binding proteins. Here we show that the 14-3-3ζ isoform interacts with both the actin-depolymerizing factor cofilin and its regulatory kinase, LIM (Lin-11/Isl-1/Mec-3)-domain-containing protein kinase 1 (LIMK1). In both yeast two-hybrid assays and glutathione S-transferase pull-down experiments, these proteins bound efficiently to 14-3-3ζ. Deletion analysis revealed consensus 14-3-3 binding sites on both cofilin and LIMK1. Furthermore, the C-terminal region of 14-3-3ζ inhibited the binding of cofilin to actin in co-sedimentation experiments. Upon co-transfection into COS-7 cells, 14-3-3ζ-specific immunoreactivity was redistributed into characteristic LIMK1-induced actin aggregations. Our data are consistent with 14-3-3-protein-induced changes to the actin cytoskeleton resulting from interactions with cofilin and/or LIMK1.

Key words: actin, actin-depolymerizing factor, cytoskeletal dynamics, testicular protein kinase 1 (TESK1).

INTRODUCTION

The 14-3-3 proteins constitute a family of highly related cytosolic 30 kDa proteins that assemble into homo- or hetero-dimers [1]. Although characterized originally as abundant acidic brain proteins [2], their expression is not restricted to neuronal tissues [3,4]. In mammals, seven 14-3-3 isoforms have been identified (β, γ, ϵ, η, σ, τ and ζ) on the basis of their differential elution from HPLC columns [5]. These isoforms show distinct expression patterns in mammalian tissues, with 14-3-3ζ being particularly abundant in the central nervous system (J. Birkenfeld, B. Schlötcke, H. Betz and D. Roth, unpublished work).

Over the last decade, numerous reports have implicated 14-3-3 proteins in a variety of cellular activities, including cell cycle regulation [6], apoptosis [7], neurotransmitter synthesis [8], neuronal development [9,10] and exocytosis [11,12]. In addition, 14-3-3 proteins have been shown to interact with enzymes that participate in signal transduction pathways. Among these are Raf1 kinase [13], Bcr-Abl [14], protein kinase C [15] and phosphoinositide 3-kinase [16]. 14-3-3 proteins bind to the majority of their ligands in a phosphoserine-dependent manner; however, phosphorylation-independent interactions have also been reported (reviewed in [3,4]). Most 14-3-3 ligands contain specific phosphorylated serine recognition sequences that are closely related to the prototypic motif R(S)$X_{1,2}$S(p)XP [where $X_{1,2}$ indicates that the motif can contain one or two amino acids at this position, and S(p) denotes phosphoserine] [3,4]. Based on the multitude of their binding partners and their involvement in numerous cellular functions, 14-3-3 dimers are thought to act as adaptor proteins which participate in the spatial organization of signalling complexes [3,17] and the subcellular localization of cargo proteins [18].

One property of 14-3-3 proteins is to stimulate regulated exocytosis in permeabilized adrenal chromaffin cells. Purified 14-3-3 proteins have been shown to reconstitute catecholamine secretion from these cells [11,19]. It is assumed that this reconstitution of catecholamine release results from a 14-3-3-mediated transient reorganization of the cortical actin network, a natural barrier that hinders the fusion of secretory granules with the plasma membrane [19,20]. 14-3-3 proteins also regulate actin organization in the yeast *Saccharomyces cerevisiae*, as revealed by the disruption of the actin cytoskeleton that is observed upon overexpression of the C-terminal region of the 14-3-3 yeast homologue Bmh2p [21]. However, the effector molecules through which 14-3-3 proteins mediate microfilament reorganization have remained enigmatic.

The actin-depolymerizing factor (ADF)/cofilin family of proteins is known to be essential for the dynamic changes in the actin cytoskeleton that occur during cell locomotion or other processes that are accompanied by a reorganization of cellular shape (for a review, see [22]). By removing actin monomers from the pointed ends of actin filaments, and by its ability to sever the latter, cofilin increases the rate of actin turnover [22]. The activity of cofilin is regulated by phosphorylation of a crucial serine residue (serine-3), which results in inactivation of its depolymerization activity [23]. Different cellular stimuli cause dephosphorylation of cofilin and thereby induce actin rearrangements that are required for neurite outgrowth [24] and the formation of lamellipodia in fibroblasts [25]. Recently we demonstrated that cofilin is also dephosphorylated during Ca^{2+}-triggered catecholamine secretion from adrenal chromaffin cells, indicating a role in regulated exocytosis [26]. LIM (Lin-11/Isl-1/Mec-3)-domain-containing protein kinases (LIMKs) are known to phosphorylate cofilin on serine-3 *in vitro* and *in vivo* [27,28], and hence are considered as key regulators of cofilin. The brain-specific LIMK1 and the ubiquitously expressed LIMK2 define a novel family of serine/threonine protein kinases [29] that exhibit a unique domain structure composed of two N-terminal LIM domains followed

Abbreviations used: ADF, actin-depolymerizing factor; GST, glutathione S-transferase; HA, haemagglutinin; HEK, human embryonic kidney; LIM domain, Lin-11/Isl-1/Mec-3 domain; LIMK, LIM-domain-containing protein kinase; PAK, p21-activated protein kinase; PDZ domain, PSD-95/Dlg/ZO-1 domain; ROCK, Rho-associated, coiled-coil-forming protein kinase; TESK, testicular protein kinase; TRITC, tetramethylrhodamine β-isothiocyanate; VSV-G, vesicular stomatitis virus glycoprotein.

[1] To whom correspondence should be addressed (e-mail neurochemie@mpih-frankfurt.mpg.de).

by a PDZ (PSD-95/Dlg/ZO-1) domain and a C-terminal kinase domain [30]. Recently this protein kinase family has been extended by testicular protein kinase 1 (TESK1) and TESK2, which both carry N-terminal protein kinase domains closely related to those of LIMKs [31]. Although LIMKs and TESKs are both capable of phosphorylating cofilin on serine-3 [27,28,32], these kinases differ in their overall domain signatures [31] and respond to different upstream signalling pathways. While the small GTPases Rho, Rac and Cdc42 stimulate the kinase activities of LIMKs through their downstream effectors Rho-associated, coiled-coil-forming protein kinase (ROCK) [33], p21-activated kinase (PAK) [34] and myotonic dystrophy kinase-related Cdc42 binding kinase α [35], TESK activities are not affected by ROCK or PAK, but are likely to be stimulated by an integrin-mediated signalling mechanism [32].

Here we used a yeast two-hybrid screen with the C-terminal region of the 14-3-3ζ isoform as bait to identify cofilin and LIMK1 as novel interaction partners of 14-3-3ζ. Interactions were confirmed biochemically and by co-localization of the respective proteins in F-actin-enriched structures of transfected COS-7 cells. Our findings are consistent with 14-3-3-induced actin reorganization processes being mediated via an actin depolymerizing factor and its regulatory kinase.

EXPERIMENTAL

Plasmid construction

Myc-tagged mouse LIMK1/Kiz-1 cDNA ([35a]; EMBL/GenBank accession number U14166) was generously provided by P. Caroni (Friedrich-Miescher-Institute, Basel, Switzerland). The generation of haemagglutinin (HA)-tagged individual fragments of LIMK1 and the fusion of full-length LIMK1 with the LexA DNA-binding domain has been described before [36]. The cDNA coding for the rat homologue of 14-3-3ζ ([36a]; EMBL/GenBank accession number D17615) was kindly provided by M. Watanabe (University of Sapporo, Japan). To generate an expression plasmid coding for C-terminally VSV-G (vesicular stomatitis virus glycoprotein)-tagged 14-3-3ζ, the cDNA was amplified by PCR using primers with a 5′ *Eco*RI overhang (forward; 5′-CTA CGT GAA TTC ATG GAT AAA AAT GAG CTG GTG CAG-3′) and a 3′ *Xba*I overhang (reverse; 5′-CTA GTC TAG ATC CCT TAC CCA GGC GGT TCA TTT CGA TAT CAG TGT A**CT CGA G**AT TTT CCC CTC CTT CTC CGC C-3′). The VSV-G epitope was included in the primer sequence of the reverse primer (underlined), which also contained an additional *Xho*I site (in bold) for removal of the 14-3-3ζ insert. The amplified PCR product was subcloned via *Eco*RI and *Xba*I restriction sites into the mammalian expression vector pcDNA3.1 (Invitrogen) (pCDNA-14-3-3ζ-VSV). A 14-3-3ζ C-terminal fragment comprising amino acids 138–246 was generated by PCR using a reverse primer with a *Sal*I overhang (5′-ata ccg gtc gac att ttc ccc tcc ttc tcc cgc ttc-3′) and a specific forward primer with an *Eco*RI overhang (see Yeast two-hybrid analysis section below). The amplified PCR product was then inserted into *Eco*RI/*Xho*I-cut pCDNA-14-3-3ζ-VSV vector. All resulting constructs were verified by DNA sequencing, and their expression was analysed in transiently transfected human embryonic kidney (HEK) 293 cell lysates by immunoblotting with anti-VSV-G antibody (Roche Inc.; results not shown).

A construct comprising maltose-binding protein fused to LIMK1 was produced by subcloning full-length LIMK1 into *Eco*RI/*Xho*I sites of the vector pMAL-C2 (New England Biolabs). Full-length cofilin was generated by PCR using the 5′-deleted clone cofilin Δ20 obtained from the two-hybrid screen as template. The PCR reaction was carried out using standard procedures with a forward primer harbouring the sequence coding for the missing 5′-terminus (5′-CTA CGG GAA TTC ATG GCC TCT GGT GTG GCT GTC TCT GAT GGA GTC ATC AAG GTG TTC AAT GAC ATG AAA GTT CGC AAG TCT TCA ACG CCA GAA GAA GTG AAG AAA CGC-3′) and a cofilin-specific reverse primer (5′-GAT GCC GAA TTC CAA AGG CTT GCC CTC CAG G-3′), which both provided 5′ *Eco*RI restriction sites. The resulting PCR products were subcloned into the two hybrid vectors pGilda and pJG4-5 (both from Origene) and into the eukaryotic expression vector pcDNA3.1 encoding a HA tag at the 5′ end of the multiple cloning site after *Eco*RI restriction. For the construction of glutathione S-transferase (GST) fusion proteins, cDNAs coding for full-length 14-3-3ζ, its C-terminal amino acids 138–246 (see yeast two-hybrid analysis), cofilin or the PDZ domain of LIMK1 (amino acids 127–321) were subcloned into pGex4T-1 (Amersham Pharmacia). All constructs were verified by DNA sequencing. Expression of the different constructs was analysed in lysates of transiently transfected HEK 293 cells by immunoblotting, or in bacterial lysates by Coomassie Blue staining.

Yeast two-hybrid analysis

For the LexA-based two-hybrid screen, a C-terminal fragment comprising amino acids 138–246 of rat 14-3-3ζ was generated by PCR using primers with *Eco*RI overhangs. The following primer pair was used: forward, 5′-CTA CGG GAA TTC AAG AAA GGA ATT GTG GAC CAG TCA CAG-3′; reverse, 5′-GAT GCC GAA TTC ATT TTC CCC TCC TTC TCC CGC TTC-3′. The resulting fragment was subcloned via its *Eco*RI restriction sites into the *Eco*RI site of the bait vector pGilda and the construct was verified by DNA sequencing. The construct was then transformed into different yeast strains provided in the two-hybrid kit (Origene) and tested for nuclear transport and transactivation activity according to standard procedures (Clontech). The two-hybrid screen of a rat brain cDNA library (Origene) using the C-terminal 109 amino acids of 14-3-3ζ (aa 138–246) as bait was performed using standard procedures (Clontech). The specificity of protein–protein interactions was assessed qualitatively by *in vivo* plate assays and quantitatively by measuring β-galactosidase activity in liquid cultures using Chlorophenol Red β-D-galactopyranoside (Roche) as substrate. The liquid culture assay was performed as described in the Clontech Yeast Protocols Handbook.

Cell culture, transfection and preparation of cell extracts

HEK 293 cells were maintained in minimum essential medium (Gibco) supplemented with 10% (v/v) fetal calf serum, 25 units/ml penicillin, 25 μg/ml streptomycin and 2 mM glutamate. Cells were transfected by lipofection using LIPOFECTAMINE 2000™ (Invitrogen) according to the manufacturer's instructions. After 36 h, cells were washed with PBS, suspended in lysis buffer [50 mM Hepes, pH 7.4, 150 mM NaCl, 1 mM dithiothreitol, 1 mM $MgCl_2$, 1 mM $MnCl_2$, 50 mM β-glycerophosphate, 5% (v/v) glycerol, 1% (v/v) Triton X-100, Phosphatase Inhibitor Cocktail I (Sigma) and Complete Protease Inhibitor Cocktail (Roche)], and incubated on ice for 1 h. After centrifugation at 20000 ***g*** for 10 min, the supernatant was dialysed against a large excess of PBS and used for GST pull-down experiments (see below).

For immunocytochemistry, COS-7 cells were grown directly on glass coverslips in Dulbecco's modified Eagle's medium containing 10% (v/v) fetal calf serum, 25 units/ml penicillin, 25 μg/ml streptomycin and 2 mM glutamate. Transfections were

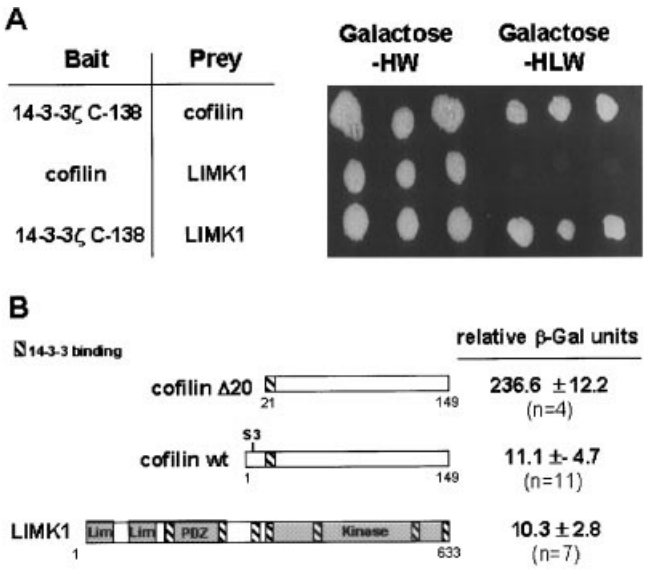

Figure 1 Pairwise yeast two-hybrid interactions of LIMK1 and cofilin with the C-terminal region of 14-3-3ζ

(**A**) *In vivo* plate assay. Yeast cells were co-transformed with pGilda-based bait vectors fused to the cDNA of cofilin or the C-terminal region of 14-3-3ζ (C-138), and pJG4-5-based prey vectors fused to the cDNAs of cofilin or LIMK1. Combinations transformed are indicated by the table on the left. Transformants grown on selective glucose media (-HW) were transferred on to inductive galactose plates containing (-HW) or lacking (-HLW) leucine and analysed for growth after 4 days at 30 °C. (**B**) β-Galactosidase liquid culture assay. Schematic representations of full-length cofilin (cofilin wt), its N-terminal deletion construct (cofilin Δ20) and LIMK1 are shown on the left. Flanking amino acid positions of the individual constructs are indicated. The distribution of putative 14-3-3 binding sites within the protein sequences is depicted by hatched boxes, and the LIMK1 phosphorylation site on cofilin (serine-3) is indicated. Results of pairwise two-hybrid analysis are shown on the right as relative β-galactosidase units. Yeast EGY48 cells harbouring the reporter plasmid pSH18-34 were co-transformed with 14-3-3ζ-(138–246) fused to the LexA DNA-binding domain together with full-length cofilin, cofilin Δ20 or LIMK1 fused to B42-AD. Single transformants grown on selective glucose plates were transferred into inductive liquid medium containing galactose and grown at 30 °C until the mid-exponential phase (A_{600} = 0.5–0.8). Cells were collected and used for β-galactosidase liquid culture assay as described in the Experimental section. The results are representative of three separate co-transformation experiments (n = number of colonies tested). Values presented are corrected for background. Note the high enzyme activity obtained for cofilin Δ20.

performed by lipofection with Fugene (Roche) according to the manufacturer's instructions.

Preparation of brain cytosol

Freshly dissected rat brains were homogenized in lysis buffer using a Polytron Potter–Elvehjem-type homogenizer. After ultracentrifugation at 100000 ***g*** for 1 h, the resulting supernatant was dialysed against a large excess of PBS. Subsequently the dialysate was centrifuged again at 100000 ***g*** for 1 h. The resulting cytosolic fraction was stored at −70 °C or used directly in GST pull-down assays.

GST pull-down assay

Affinity isolation experiments were carried out with GST fusion proteins containing full-length 14-3-3ζ (GST–14-3-3ζ) or the 14-3-3ζ C-terminus comprising amino acids 138–246 [GST–14-3-3ζ-(138–246)]. The fusion proteins were expressed in BL21pLysS cells (Invitrogen) and purified according to the manufacturer's instructions (Amersham Pharmacia). Aliquots of 20 μg of GST fusion protein or GST alone were incubated with lysate from transiently transfected HEK 293 cells (approx. 100 μg of total protein) or rat brain cytosol (approx. 300 μg of total protein) in a total volume of 250 μl of PBS overnight at 4 °C on a rocking platform. After the addition of 15 μl of glutathione–Sepharose beads and further incubation for 2 h at 4 °C, beads were recovered by centrifugation, washed five times with 500 μl of PBS, dissolved in sample buffer, subjected to SDS/PAGE on 12 % (w/v) polyacrylamide gels and subsequently immunoblotted.

In vitro transcription and translation

[^{35}S]Methionine-labelled cofilin was synthesized from the pcDNA3.1 cofilin expression construct (see above) by using a coupled transcription/translation kit (Promega) according to the manufacturer's instructions. Aliquots of the reaction mixture were used directly for actin co-sedimentation experiments (see below).

Actin co-sedimentation assay

The *in vitro* binding of GST–14-3-3ζ, GST–14-3-3ζ-(138–246) and GST–cofilin to actin was examined using an Actin Binding Protein Biochem Kit (Cytoskeleton). In brief, GST fusion proteins (approx. 5 μM) were incubated alone or together with F-actin (15 μM) in the supplied buffer for 30 min at 24 °C. Subsequently, samples were centrifuged at 110000 ***g*** for 2 h at 24 °C. Supernatant and pellets were transferred into equal volumes of 1 × SDS sample buffer and subjected to SDS/PAGE. As an alternative method, 10 μl of *in vitro*-translated ^{35}S-labelled cofilin was incubated with actin in the presence of either GST or GST–14-3-3ζ and processed as before. Proteins were detected by either Coomassie Blue staining or immunoblotting with anti-GST (Sigma) or anti-cofilin (Cytoskeleton) antibodies, or by autoradiography.

Antibodies

Antibodies against LIMK1 were raised in New Zealand White rabbits by immunization with a fusion protein of GST coupled to the PDZ domain of LIMK1 (comprising amino acids 127–321). A 500 μg portion of fusion protein was mixed with an equal volume of Freund's adjuvant, and rabbits were injected subcutaneously at multiple sites. Rabbits were given two booster injections, and were bled 2 weeks after the second boost. Later bleeds were taken 2 weeks after re-boosting. Serum was prepared as described [37] and stored at − 20 °C.

Monoclonal antibodies against c-Myc (clone 9E10; dilution for immunocytochemistry 1:50), HA (clone 12CA5; 1:250) and VSV-G (clone P5D4; 1:500) epitopes were all obtained from Roche. A polyclonal antibody against the HA epitope (dilution 1:250) was purchased from Sigma, and a polyclonal antibody against 14-3-3ζ (C16; dilution 1:500) was from Santa Cruz. Secondary Alexa antibodies were obtained from Molecular Probes.

Immunocytochemistry

Approx. 36 h after transfection, transfected cells were fixed in 4 % (w/v) paraformaldehyde for 15 min at room temperature. For single transfections, fixed cells were washed in PBS, permeabilized and incubated with primary antibodies for 1 h at room temperature. Antibodies were diluted as indicated in PBT [PBS containing 5 % (w/v) BSA and 0.25 % (v/v) Triton X-100]. Cells were then washed three times with PBT and incubated with

Alexa 488-conjugated goat anti-mouse antibody (1:250 dilution), together with FITC–phalloidin (25 nM final concentration; Sigma) to counterstain for filamentous actin, for 1 h in the dark. In case of double transfections, cells were incubated first with both the first primary antibody and Alexa 594-conjugated goat anti-rabbit/mouse antibody (1:250 dilution). After 1 h, cells were washed three times with PBT and subsequently incubated for 1 h in the dark with the second primary antibody in combination with Alexa 488-conjugated goat anti-mouse/rabbit secondary antibody. In both cases, coverslips were then washed again, rinsed in water and mounted in Mowiol (Roche). Pictures were taken with a fluorescence microscope (Zeiss) connected to a digital camera system using Metamorph software (Invisitron).

RESULTS

Identification of cofilin and LIMK1 as 14-3-3ζ-interacting proteins

In order to identify novel interaction partners of 14-3-3 proteins that may be involved in actin organization processes, the C-terminal region (amino acids 138–246) of 14-3-3ζ was fused in-frame to the LexA DNA-binding domain of the pGilda vector and used as bait to screen a rat brain cDNA library. The C-terminus was used to increase the specificity of the screen for new interaction partners, since this region of 14-3-3 proteins is not involved in dimerization, but comprises parts of the general binding groove for putative interactors and includes the most variant amino acids within the entire protein [3].

Transformants were selected for leucine prototrophy and β-galactosidase activity, as indicated by the blue colour of colonies. Upon screening 4×10^6 yeast clones, 58 clones remained positive for β-galactosidase activity after retransformation of the isolated DNAs. Nucleotide sequence analysis revealed that one of the clones represented an N-terminally truncated version of the actin depolymerizing factor cofilin which lacked the first 19 amino acids after the initiator methionine. Interestingly, this clone (named cofilin Δ20) started with a perfect 14-3-3 interaction site (R^{21}KSSTP^{26}) matching the consensus binding sequence R(S)$X_{1,2}$S(p)XP for 14-3-3 ligands [3,4]. Therefore this clone appeared to be a promising candidate to provide the missing link between 14-3-3 proteins and induced actin reorganization processes.

Yeast cells co-expressing the 14-3-3ζ C-terminal fragment 14-3-3ζ-(138–246) and full-length cofilin grew on media lacking leucine, indicating a specific interaction of the 14-3-3ζ C-terminus with the full-length cofilin protein (Figure 1A). As one of the primary functions of 14-3-3 adaptor proteins is to mediate protein–protein interactions important for the assembly of multiprotein signalling complexes [3], we examined whether 14-3-3ζ also interacts with cofilin's key regulator, LIMK1. To this end, full-length LIMK1 (amino acids 1–633) was fused in-frame to the B42 transactivation domain of vector pJG4-5 (LIMK1) and tested for interaction with GST–14-3-3ζ-(138–246) and full-length cofilin by pairwise yeast two-hybrid analysis. Growth of yeast cells on medium lacking leucine indicated interactions between GST–14-3-3ζ-(138–246) and both LIMK1 and cofilin. In

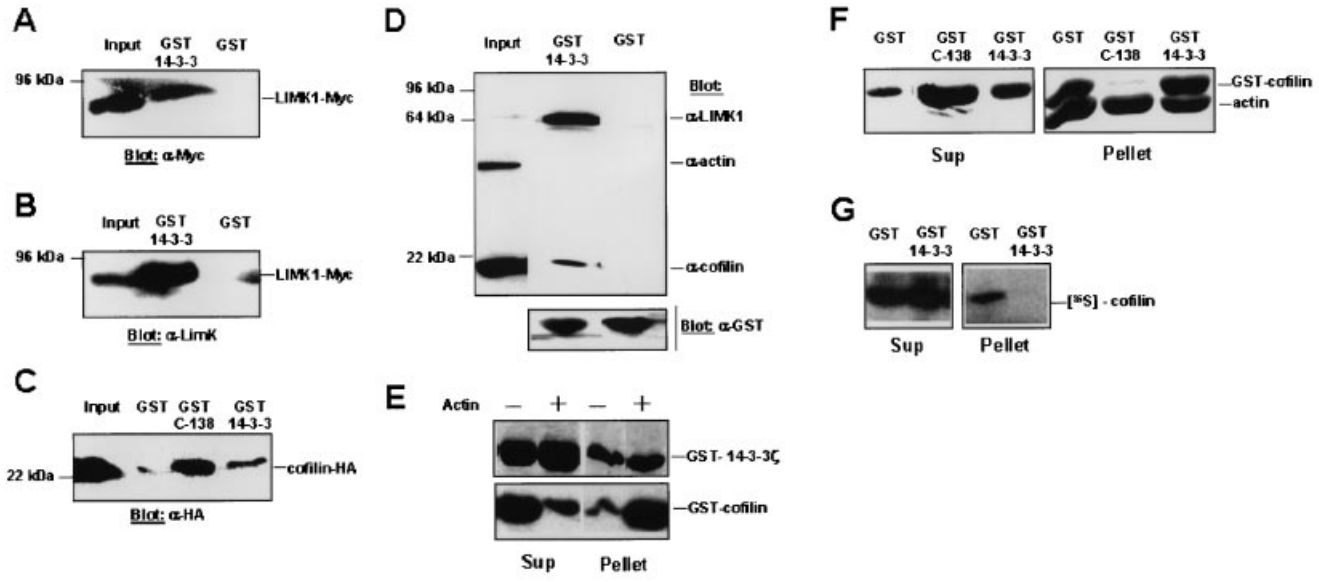

Figure 2 Binding of 14-3-3ζ to cofilin and LIMK1

GST pull-down assays with cell lysates of transfected HEK 293 cells (**A**–**C**) or rat brain cytosol (**D**, **E**). (**A**, **B**) Lysates from LIMK1–Myc-transfected HEK 293 cells were incubated with GST–14-3-3ζ or GST, followed by glutathione–Sepharose beads. After washing, bound proteins were eluted, separated by SDS/12%-PAGE and visualized by immmunoblotting with anti-Myc (α-Myc) (**A**) or anti-LIMK1 (**B**) antibodies. (**C**) Similar GST pull-down assay showing HA-tagged cofilin in lysates bound and eluted from immobilized GST proteins fused to full-length 14-3-3 ζ (GST–14-3-3) or its C-terminal region (GST C-138), or from GST alone. Note that 14-3-3ζ-(138–246) (GST C-138) bound more cofilin than did GST-14-3-3. (**D**) Freshly prepared cytosol from rat brain was incubated with GST-14-3-3 or GST, followed by glutathione–Sepharose beads. Bound proteins were analysed by Western blotting using antibodies against cofilin, actin or LIMK1 after cutting the blot into three pieces corresponding to the expected migration positions of these proteins. Equal loading of GST–protein constructs was monitored by immunoblotting with anti-GST antibody (lower panel). Note the high enrichment of LIMK1 in samples containing GST–14-3-3ζ. Positions of marker proteins are indicated in kDa on the left. (**E**) Co-sedimentation of GST–14-3-3ζ and GST–cofilin with F-actin. GST fusion proteins were incubated with (+) or without (−) filamentous actin prior to ultracentrifugation. Equivalent aliquots of the supernatant (Sup) and pellet fractions were subjected to SDS/PAGE for Coomassie Blue staining (GST–14-3-3ζ) or immunoblotting with an anti-GST antibody (GST–cofilin). Note that sedimentation of GST–14-3-3ζ was not altered by F-actin. (**F**) Co-sedimentation of GST–cofilin in the presence of GST, GST–14-3-3ζ-(138–246) (GST C-138) or GST–14-3-3ζ. Note that GST–14-3-3ζ-(138–246) inhibited the redistribution of GST–cofilin into the actin pellet. (**G**) Co-sedimentation of ^{35}S-labelled cofilin (10 μl) in the presence of either GST or GST–14-3-3ζ.

contrast, cells co-expressing LIMK1 and full-length cofilin fused to the B42 transactivation domain did not grow, indicating that LIMK1 and cofilin do not interact directly with each other in the yeast two-hybrid assay (Figure 1A). These findings indicate specific interactions of the 14-3-3ζ C-terminus with both cofilin and LIMK1. This is consistent with the existence of consensus 14-3-3 binding motifs in both proteins (Figure 1B).

When examining the efficiencies of these two-hybrid interactions by determining β-galactosidase activities using the quantitative Chlorophenol Red β-D-galactopyranoside assay (Figure 1B), cofilin and LIMK1 displayed comparable binding activities for GST–14-3-3ζ-(138–246). Surprisingly, however, cofilin Δ20 produced about 20-fold higher enzyme activities with the C-terminal fragment of 14-3-3ζ than did the full-length protein. These results suggest that the putative 14-3-3 interaction site RKSSTP of cofilin participates in binding to 14-3-3ζ, and that this interaction is negatively regulated by the preceding N-terminal region. However, our data do not exclude the possibility that additional points of contact may exist between 14-3-3ζ and cofilin.

Biochemical verification of two-hybrid interactions

Interactions between cofilin, LIMK1 and 14-3-3ζ were then tested by GST pull-down assays. Cell lysates from HEK 293 cells transfected with Myc-tagged LIMK1 or HA-tagged cofilin were incubated with GST, GST–14-3-3ζ-(138–246) or GST–14-3-3ζ fusion proteins. Immunoblot analysis of the bound proteins with anti-Myc and anti-LIMK1 antibodies demonstrated that LIMK1 bound to immobilized GST–14-3-3ζ, but not to GST (Figures 2A and 2B). Only weak binding was observed when GST–14-3-3ζ-(138–246) was used in LIMK1 binding assays (results not shown). In addition, the same GST pull-down assay showed that HA-tagged cofilin interacted with both GST–14-3-3ζ and GST–14-3-3ζ-(138–246), but not with GST alone (Figure 2C). Interestingly, greater binding of HA–cofilin was obtained with the C-terminal region of 14-3-3ζ [GST–14-3-3ζ-(138–246)] than with full-length 14-3-3ζ.

To demonstrate interactions of 14-3-3ζ with LIMK1 and cofilin in native tissue, GST pull-down experiments were carried out with cytosol from rat brain. Immunoblot analysis with antibodies against cofilin, LIMK1 and actin disclosed the presence of LIMK1 and cofilin on beads loaded with GST–14-3-3ζ, but not GST. Furthermore, GST–14-3-3ζ markedly enriched LIMK1, but not cofilin, from the cytosol (Figure 2D). This suggests that LIMK1 binds more avidly to GST–14-3-3ζ than does cofilin. Control experiments showed that immunodetection by our anti-LIMK1 antibody was highly specific, as pre-incubation with a fusion protein comprising maltose-binding protein and LIMK1 blocked all staining (results not shown).

The interactions of 14-3-3ζ with LIMK1 and cofilin seemed to be independent of actin, since actin was not found in the bound protein complexes (Figure 2D). Furthermore, co-sedimentation experiments with filamentous actin failed to detect a specific association of GST–14-3-3ζ with microfilaments. Figure 2(E) shows that GST–cofilin co-sedimented with F-actin. In contrast, no co-sedimentation of GST–14-3-3ζ (Figure 2E) or GST (results not shown) was observed, indicating that 14-3-3ζ does not bind F-actin. Next we tested whether the actin-binding properties of cofilin are altered in the presence of GST–14-3-3ζ or GST–14-3-3ζ-(138–246) (Figure 2F). Interestingly, when GST–14-3-3ζ-(138–246), but not GST, was added to the F-actin co-sedimentation assay, cofilin no longer co-sedimented with actin filaments, but was mainly retained in the supernatant. Full-length GST–14-3-3ζ also increased the amount of GST–cofilin in the supernatant, albeit to a lesser extent (Figure 2F). The GST–14-3-3ζ-induced inhibition of the cofilin–actin interaction was even more evident when actin co-sedimentation assays were performed with *in vitro*-translated [^{35}S]methionine-labelled cofilin instead of the bacterially produced GST–cofilin (Figure 2G). Under these conditions, only a minor fraction of the *in vitro*-synthesized cofilin displayed actin-binding competence, as revealed by redistribution into the pellet upon co-sedimentation with F-actin (results not shown). The amount of co-sedimentable ^{35}S-labelled cofilin was not altered in the presence of GST, but upon addition of GST–14-3-3ζ ^{35}S-cofilin was no longer detectable in the actin pellet (Figure 2G). Together, these results suggest that interactions with the C-terminal region of 14-3-3ζ inhibit the binding of cofilin to F-actin.

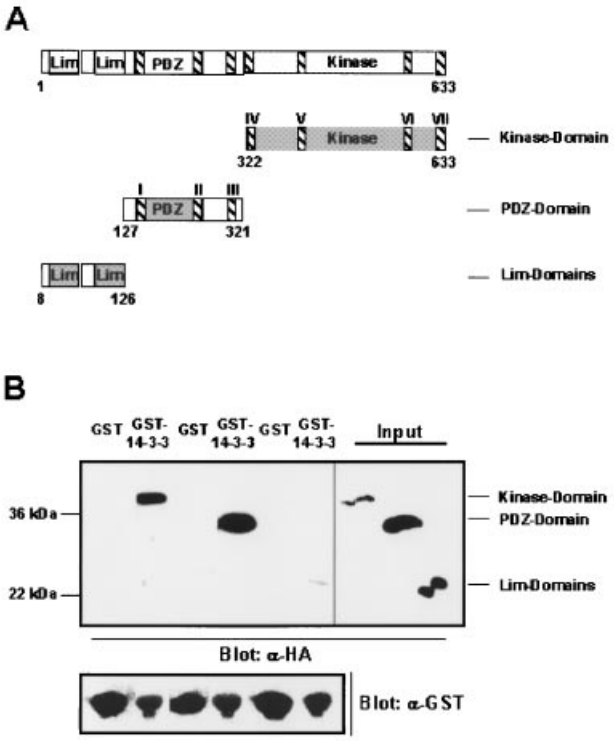

Figure 3 Interaction of 14-3-3ζ with individual domains of LIMK1

(**A**) Schematic representation of the LIMK1 domains analysed. Numbers indicate the flanking amino acid positions of the constructs used. Putative 14-3-3 binding sites within the protein sequences are indicated by hatched boxes and Roman numbers. The positions of the putative 14-3-3 binding sites are: I, R^{162}GLSVIDP^{169}; II, R^{281}SCSID^{286}; III, R^{306}SESL^{310}; IV, R^{321}PSDL^{325}; V, R^{423}VSFA^{427}; VI, R^{580}PSFV^{584}; VII, R^{620}GESSLP^{626}. (**B**) GST pull-down assay showing interactions of 14-3-3ζ with the PDZ and kinase domains of LIMK1. HA-tagged individual domains of LIMK1 were transiently transfected into HEK 293 cells. Lysates of the transfected cells were incubated with GST–14-3-3 or GST, followed by glutathione–Sepharose beads, and bound proteins were analysed by immunoblotting with anti-HA antibody (α-HA). GST protein loading was examined by immunoblotting with anti-GST antibody (lower panel). Positions of marker proteins are indicated in kDa on the left.

14-3-3ζ interacts with the PDZ domain and the kinase domain of LIMK1

Previous studies have shown that 14-3-3 proteins bind preferentially to motifs resembling the R(S)X$_{1,2}$S(p)XP motif [3,17] containing a central phosphorylated serine. LIMK1 exhibits

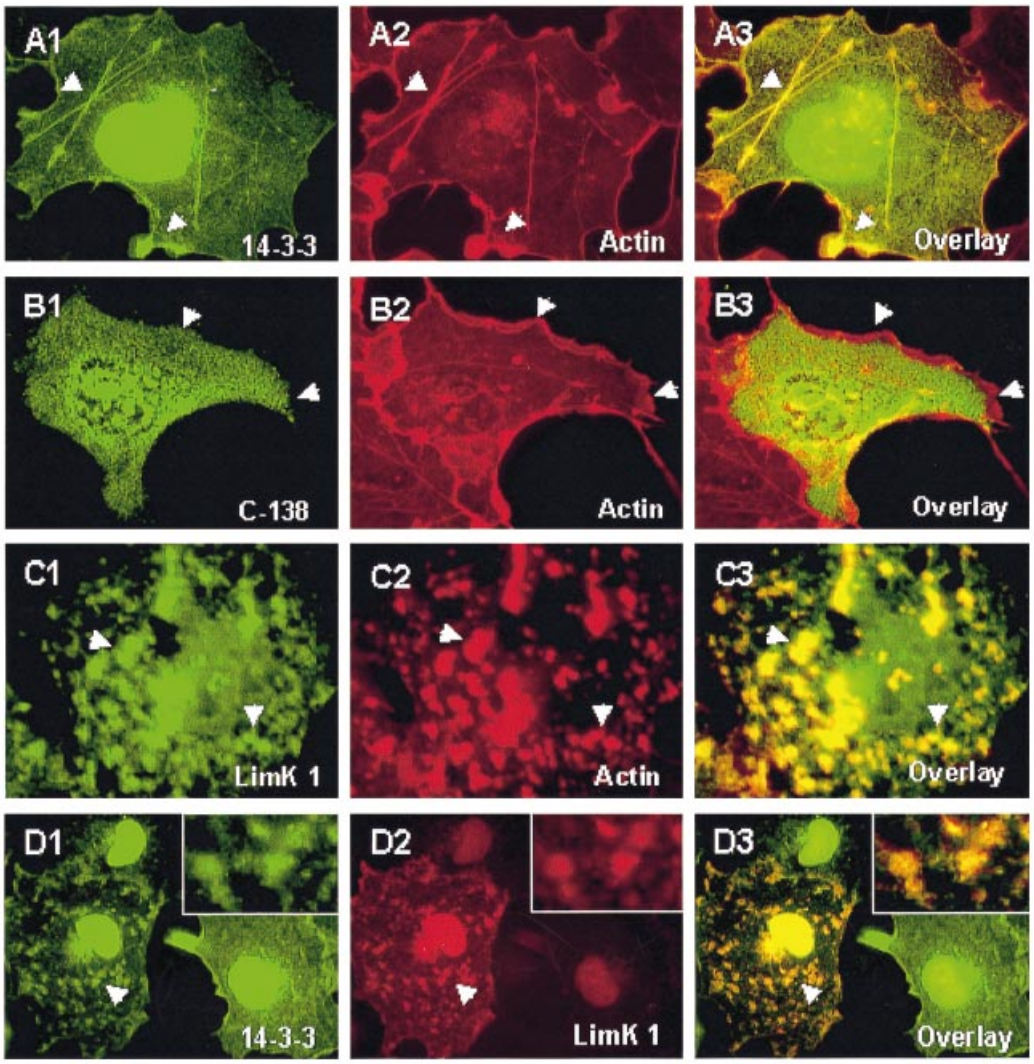

Figure 4 Co-localization of 14-3-3 with actin, cofilin and LIMK1 in COS-7 cells

(**A**)–(**C**) Co-localization of 14-3-3ζ, 14-3-3ζ-(138–246) (C-138) and LIMK1 with F-actin-enriched structures. COS-7 cells were singly transfected with plasmids carrying the cDNA sequences for 14-3-3–VSV-G, 14-3-3ζ-(138–246)–VSV-G or Myc–LIMK1. After 36 h in culture, cells were fixed and the expressed proteins were visualized using their epitope tags (**A1**–**C1**; green channel). Nuclear staining resulted from secondary antibodies and thus represents an artefact of the immunostaining procedure. In addition, cells were counterstained for filamentous actin with TRITC/phalloidin (**A2**–**C2**; red channel). Yellow fluorescence in the overlay images results from superposition of green and red channels. Arrowheads indicate selected regions of co-localization with actin (**A**, **C**) or F-actin-rich regions that are devoid of 14-3-3ζ-(138–246)–VSV-G immunoreactivity (**B**). (**D**) Co-localization of 14-3-3ζ with LIMK1. COS-7 cells co-transfected with 14-3-3–VSV-G and Myc–LIMK1 were cultured for 36 h, fixed and stained with anti-14-3-3 (**D1**) or anti-Myc (**D2**) antibodies respectively. Selected regions of co-localization (arrowheads) are shown at higher magnification (**D3**, insets).

seven potential binding sites for 14-3-3 proteins that are located within and around the PDZ domain and the kinase domain regions (Figure 3A). To determine whether these regions are implicated in interactions with 14-3-3 proteins, we conducted a series of GST pull-down assays with lysates from transfected HEK 293 cells expressing HA-tagged subdomains of LIMK1 (Figure 3A). We found strong binding of GST–14-3-3ζ to the PDZ and the kinase domains, whereas no interaction was observed with the LIM1/2 domain (Figure 3B). These results correlate with the distribution of potential 14-3-3 binding sites, as only the LIM1/2 domain, which is devoid of putative interaction motifs, was not detected in GST–14-3-3ζ precipitates. Therefore binding of 14-3-3ζ to LIMK1 involves multiple motifs localized within distinct domains of LIMK1.

Co-localization of 14-3-3ζ with LIMK1 in transfected COS-7 cells

In vivo interactions of 14-3-3ζ with cofilin and LIMK1 were tested by expressing tagged versions of the polypeptides in transfected COS-7 cells. Immunofluorescent staining showed that, upon single transfection, 14-3-3ζ–VSV-G immunoreactivity was concentrated at the periphery of cells (Figure 4A1). In addition, fibre-like structures within the cytosol as well as diffuse cytoplasmic staining were detected. Labelling of F-actin with tetramethylrhodamine β-isothiocyanate (TRITC)/phalloidin (Figure 4A2) revealed that F-actin staining coincided with the submembranous and filamentous 14-3-3ζ–VSV-G staining (Figure 4A3), indicating that 14-3-3ζ co-localizes with F-actin-enriched structures. In contrast, 14-3-3ζ-(138–246)–VSV-G

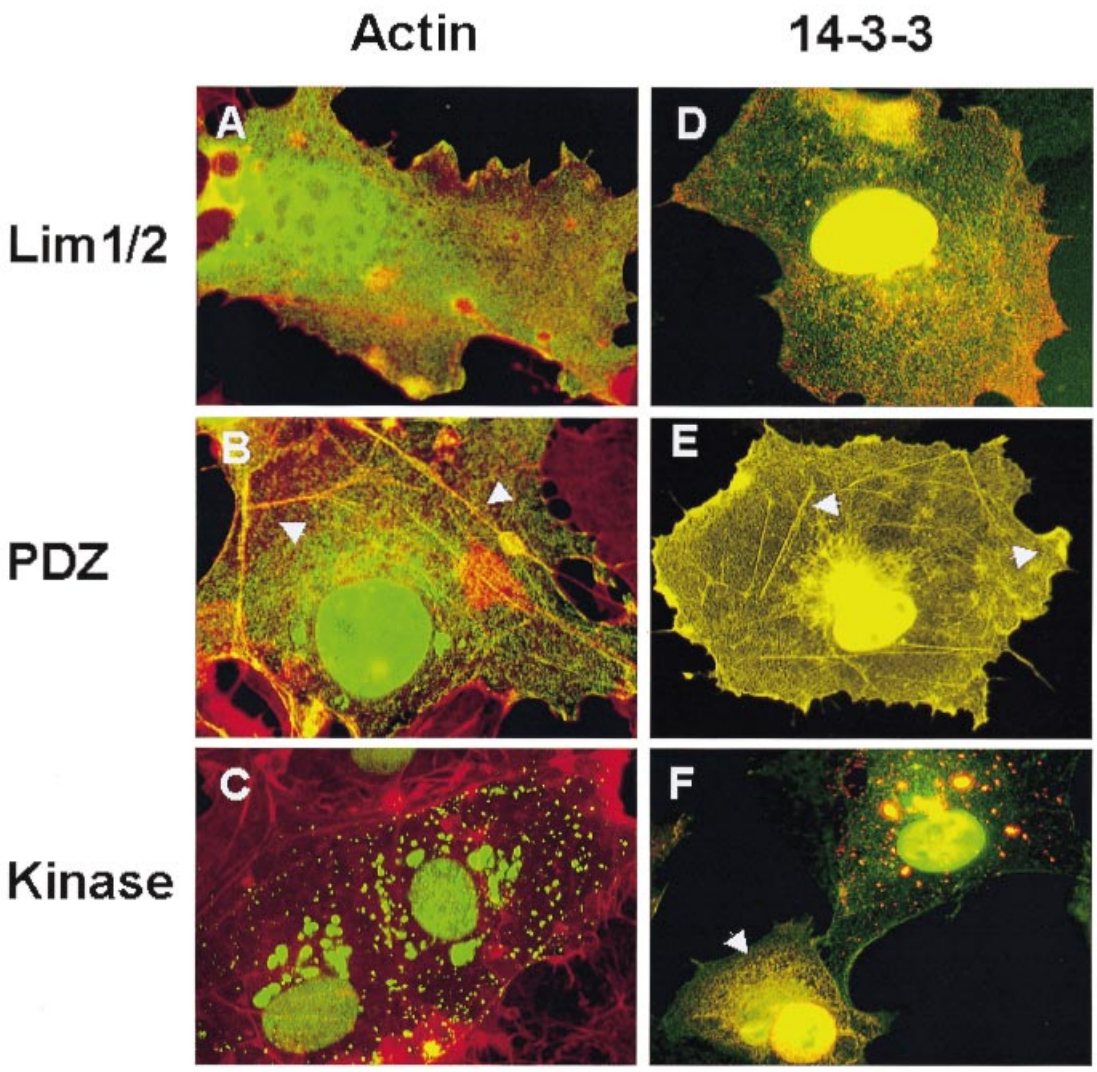

Figure 5 Co-localization of individual LIMK1 domains with actin and 14-3-3 in COS-7 cells

COS-7 cells were either singly transfected with cDNAs coding for HA-tagged versions of the individual LIMK1 domains (Actin panels) or co-transfected with these cDNAs plus 14-3-3ζ–VSV-G (14-3-3 panels). After 36 h in culture, cells were fixed and stained for the epitope tags. In the case of singly transfected cells (**A**–**C**), cells were counterstained for filamentous actin with TRITC/phalloidin (red channel). Arrowheads indicate co-localization (yellow) of the LIMK1 PDZ domain with stress fibres. In doubly transfected cells (**D**–**F**), both the LIMK1 PDZ and kinase domains (red) co-localized with 14-3-3ζ–VSV-G (green). Arrowheads point to doubly stained stress fibres (**E**) and to cells that no longer contain the characteristic kinase clusters found routinely upon co-transfection with 14-3-3ζ (**F**).

showed no obvious co-localization with actin cables and was mainly excluded from protrusive membrane structures and submembraneous F-actin-rich regions (Figures 4B1–4B3). Thus co-localization with F-actin may involve the N-terminal region of 14-3-3ζ. Alternatively, since 14-3-3 proteins dimerize via their N-termini [1], dimer integrity may be essential for the recruitment of 14-3-3 proteins to microfilamental structures.

Overexpression of LIMK1 alone resulted in a loss of actin stress fibres and the appearance of large actin aggregates (Figures 4C1–4C2), a phenomenon noted previously by Edwards and Gill [38]. Furthermore, LIMK1 immunoreactivity was co-localized with these actin aggregates (Figure 4C3). Upon co-expression of 14-3-3ζ–VSV-G (Figure 4D1) with Myc–LIMK1 (Figure 4D2), 14-3-3ζ was re-localized from a diffuse cytoplasmic distribution accompanied by filament staining to typical actin/LIMK1 aggregates (Figure 4D3; see inset). This re-localization of 14-3-3ζ upon LIMK1-induced changes in the actin cytoskeleton underlines the relevance of the protein interactions observed *in vitro*, and suggests that they function in actin organization processes.

We also tried to visualize co-localization of HA–cofilin and 14-3-3ζ–VSV-G on F-actin-enriched structures in transfected cells. However, these experiments proved difficult, since overexpression of cofilin is known to cause a complete loss of F-actin staining [22]. This presumably reflects competition between cofilin and phalloidin for F-actin binding sites [22]. Here, co-localization of 14-3-3ζ and cofilin on microfilaments was seen at low expression levels (results not shown). With increasing protein levels of cofilin, cellular F-actin staining disappeared, and cofilin and 14-3-3ζ immunoreactivities both showed a uniform cytoplasmic distribution (results not shown).

Co-expression of 14-3-3ζ with subdomains of LIMK1

To unravel whether the interactions between 14-3-3ζ and the PDZ and kinase domains of LIMK1 observed *in vitro* (Figure 3) are also detectable under *in vivo* conditions, HA-tagged versions of the LIM1/2, PDZ and kinase domains of LIMK1 were expressed in COS-7 cells and their distributions visualized by immunostaining (Figure 5). Co-localization with the actin cytoskeleton was revealed using fluorescently labelled phalloidin (Figures 5A–5C). Fluorescence microscopy showed that the LIM1/2 domain of LIMK1 was distributed throughout the cytosol and not localized to actin filaments (Figure 5A). In contrast, the PDZ domain co-localized exactly with actin stress fibres, as indicated by yellow fluorescence upon merging of the green and red channels (Figure 5B). Expression of the kinase domain of LIMK1 resulted in the formation of aggregates, as demonstrated by a punctate staining frequently seen in perinuclear areas (Figure 5C). These aggregates were not stained by phalloidin, indicating that they were devoid of actin. Consistent with this interpretation, microfilaments were clearly visible in these kinase-domain-transfected cells. Similar results have been described by others and are assumed to reflect incomplete folding of the kinase domain [38]. Co-expression of 14-3-3ζ had no influence on the distribution of the LIM1/2 domain, as both proteins showed wide cytosolic distributions (Figure 5D). When expressed in combination with the PDZ domain of LIMK1, 14-3-3ζ co-localized with PDZ-domain-stained structures, i.e. actin stress fibres and submembranous actin condensations (Figure 5E). Co-expression of 14-3-3ζ and the kinase domain of LIMK1 caused the formation of 14-3-3ζ- and kinase-domain-positive aggregates (Figure 5F). Notably, the fraction of cells exhibiting such clusters was markedly reduced to about 25% as compared with singly transfected cells, of which close to 100% contained kinase domain clusters (Figure 5F and results not shown). In conclusion, these immunofluorescence data confirm our biochemical results by demonstrating that 14-3-3ζ associates with LIMK1 *in vivo*.

DISCUSSION

In the present study we have identified the ADF cofilin and its key regulatory protein LIMK1 as novel interactors with the C-terminal region of 14-3-3ζ. These interactions, originally disclosed in the yeast two-hybrid system, were confirmed for full-length 14-3-3ζ *in vitro* by using a GST–14-3-3ζ fusion protein, and are consistent with the presence of consensus 14-3-3 binding motifs in both proteins. Cofilin possesses a single 14-3-3 binding sequence in its N-terminal region which, in two-hybrid assays, proved particularly accessible upon truncation of the preceding 20 amino acid residues. In contrast, LIMK1 contains seven predicted 14-3-3 interaction motifs that are localized in and around its PDZ and kinase domains. Their distribution correlates with the *in vitro* binding properties of the individual subdomains, since the isolated PDZ and kinase domains interacted with 14-3-3ζ in the GST pull-down assay, whereas the LIM1/2 domain, which lacks such motifs, failed to bind under the same conditions. The reasons for the occurrence of multiple 14-3-3 binding sites in LIMK1 are presently unclear, but may reflect differential regulation of the functions of these domains by distinct 14-3-3 proteins.

Dimeric 14-3-3 proteins have been shown to regulate numerous cellular functions, including cell cycle control, signal transduction, apoptosis and exocytosis (for reviews, see [3,4]). By binding to diverse partner proteins, 14-3-3 adaptor proteins facilitate protein–protein interactions implicated in the spatial organization of signalling complexes, the modulation of enzyme activities and the subcellular compartmentalization of distinct effector proteins. In addition, 14-3-3 proteins bind to distinct components of the cytoskeleton [39–41] and affect the structure of microfilaments [20,21]. In permeabilized adrenal chromaffin cells, 14-3-3 proteins stimulate calcium-dependent exocytosis by reorganization of the cortical actin belt underlying the plasma membrane [11,20]. Similarly, in *Saccharomyces cerevisiae*, overexpression of the C-terminal region of the yeast 14-3-3 homologue Bmh2p has been shown to disrupt the actin cytoskeleton, resulting in vesicle targeting defects [21]. Our data indicate that interactions with cofilin and LIMK1 may underlie these effects of 14-3-3 proteins on microfilaments.

Despite repeated attempts, we have not been able to demonstrate *in vitro* binding of recombinant 14-3-3 to F-actin preparations. However, upon transfection in COS-7 cells, full-length epitope-tagged 14-3-3ζ was associated with actin filaments. Notably, the N-terminally truncated fragment comprising residues 138–246 of 14-3-3ζ failed to co-localize with polymerized actin, although it displayed high-affinity interactions with both cofilin and LIMK1 in GST pull-down assays and/or the yeast two-hybrid system. The N-terminal domain of 14-3-3 proteins is known to be required for dimer formation [3,4]. Thus dimerization could be a prerequisite for efficient recruitment of 14-3-3 proteins to actin via cofilin or LIMK1. However, in an actin co-sedimentation assay in the presence of cofilin, both recombinant 14-3-3ζ and the 14-3-3ζ-(138–246) construct did not bind F-actin, but rather inhibited cofilin binding to the F-actin pellet. This suggests that recruitment of 14-3-3 proteins to the actin cytoskeleton *in vivo* must involve actin-binding proteins other than cofilin.

For LIMK1, a role in 14-3-3ζ recruitment to microfilaments appears more likely, although no direct evidence for respective interactions could be obtained. Due to inherent difficulties in generating the full-length recombinant kinase, actin co-sedimentation experiments, as done with cofilin, proved difficult for LIMK1 (J. Birkenfeld, unpublished work). Biochemical evidence for LIMK1-mediated binding of 14-3-3ζ to F-actin is therefore lacking. In co-transfection experiments, 14-3-3ζ–VSV-G showed perfect co-localization with LIMK1-enriched cytoplasmic actin accumulation, and a similar co-distribution with microfilaments was also seen for the isolated PDZ domain of the enzyme. On the other hand, and consistent with the GST pull-down data, 14-3-3ζ–VSV-G co-localized with the cytosolic aggregates formed by the isolated kinase domain of LIMK1, although these aggregates did not contain F-actin, as revealed by a lack of phalloidin staining. Thus 14-3-3ζ clearly interacts in a cellular context with binding motifs of LIMK1. Whether the latter are essential for the enrichment of 14-3-3 immunoreactivity on F-actin structures remains to be determined.

LIMK is known to regulate the organization of the actin cytoskeleton by phosphorylating cofilin, and thereby inhibiting its actin-binding and depolymerizing activities [27,28]. Thus the direct interaction of 14-3-3 proteins with LIMK1 could prevent kinase action on microfilament-bound cofilin, and thereby alter the dynamics of the actin cytoskeleton. Alternatively, the LIMK1-induced recruitment of 14-3-3ζ–VSV-G to F-actin-rich structures could be indicative of an adaptor role for 14-3-3 that facilitates binding, and hence phosphorylation, of the substrate cofilin. However, in our hands preliminary *in vitro* kinase experiments failed to reveal LIMK1-induced changes in the phosphorylation of cofilin upon addition of recombinant 14-3-3ζ (J. Birkenfeld, unpublished work), although a recent study demonstrating an interaction between the LIMK1-related kinase TESK1 and 14-3-3β has disclosed a negative regulation of cofilin

phosphorylation by TESK1 in the presence of 14-3-3β [42]. Negative regulation of cofilin activity could also arise from the sequestration of inactive (phosphorylated) cofilin by 14-3-3 proteins. In view of the plethora of 14-3-3 binding partners identified, we presently favour the idea that a complex network of 14-3-3 interactions with LIMK1, cofilin and additional 14-3-3 binding proteins allows for an orchestrated sequestration, and thereby regulation, of different actin regulatory proteins.

In our co-expression studies, 14-3-3ζ not only co-localized with, but also decreased the formation of, LIMK1 kinase domain folding aggregates in COS-7 cells. This may be indicative of improved domain folding upon 14-3-3 binding; indeed, chaperone-like functions have been assigned to 14-3-3 proteins previously. Upon co-transfection in 293 cells, 14-3-3η has been shown to solubilize large fractions of cytoplasmic A20 aggregates to more diffusely distributed punctae [43]. Furthermore, co-expression of 14-3-3η reduced the extent of cytoplasmic p190-RhoGEF aggregate formation in Neuro 2a cells [44]. In addition to serving as adaptor and sequestering proteins, the different members of the 14-3-3 family thus may also act by assisting protein folding.

In conclusion, our data suggest a complex network of interactions between 14-3-3ζ, cofilin and LIMK1 in the regulation of actin dynamics. Unravelling the physiological regulation and precise functions of these interactions should help to further elucidate how cytoskeletal reorganization contributes to cellular growth, differentiation and neurotransmitter secretion.

We thank Dr Bertram Schmitt for support and advice, Bärbel Kohler for excellent technical assistance and Maren Baier for help with the preparation of the manuscript. This study would not have been possible without the 14-3-3ζ and LIMK1/Kiz-1 clones provided by Dr M. Watanabe (Sapporo, Japan) and Dr P. Caroni (Friedrich-Miescher-Institute, Basel, Switzerland) respectively. This work was supported by grants from Deutsche Forschungsgemeinschaft (to D.R.) and by Fonds der Chemischen Industrie (to H.B.). J.B. is a member of the Graduiertenkolleg Neuronale Plastizität.

REFERENCES

1 Aitken, A., Collinge, D. B., van Heudsen, B. P., Isobe, T., Roesenboom, P. H., Rosenfeld, G. and Soll, J. (1992) 14-3-3 proteins: a highly conserved, widespread family of eukaryotic proteins. Trends Biochem. Sci. **17**, 498–501

2 Moore, B. and Perez, V. J. (1967) Specific acidic proteins of the nervous system. In Physiological and Biochemical Aspects of Nervous Integration (Carlson, F. D., ed.), pp. 343–359, Prentice-Hall, Englewood Cliffs, NJ

3 Aitken, A. (1996) 14-3-3 proteins on the MAP. Trends Cell Biol. **6**, 341–347

4 Fu, H., Subramanian, R. R. and Masters, S. C. (2000) 14-3-3 proteins: structure, function and regulation. Annu. Rev. Pharmacol. Toxicol. **40**, 617–647

5 Ichimura, T., Isobe, T., Okuyama, T., Takahashi, N., Araki, K., Kuwano, R. and Takahashi, Y. (1988) Molecular cloning of cDNA coding for brain specific 14-3-3 protein, a protein kinase dependent activator of tyrosine and tryptophan hydroxylases. Proc. Natl. Acad. Sci. U.S.A. **85**, 7084–7088

6 Peng, C. Y., Graves, P. R., Thomas, R. S., Wu, Z., Shaw, A. S. and Piwnica-Worms, H. (1997) Mitotic and G2 checkpoint control: regulation of 14-3-3 binding by phosphorylation of Cdc25C on Serine-2126. Science **277**, 1501–1505

7 Zha, J., Harda, H., Yang, E., Jockel, J. and Korsmeyer, S. J. (1996) Serine phosphorylation of death agonist BAD in response to survival factor results in binding to 14-3-3 not BCL-X(L). Cell **87**, 619–628

8 Ichimura, T., Isobe, T., Okuyama, T., Yamauchi, T. and Fujisawa, H. (1987) Brain 14-3-3 protein is an activator of protein that activates tryptophan 5-monooxygenase and tyrosine 3-monooxygensae in the presence of Ca^{2+}, calmodulin-dependent kinase II. FEBS Lett. **219**, 79–82

9 Chang, H. C. and Rubin, G. M. (1997) 14-3-3ϵ positively regulates Ras1 mediated signalling in Drosophila. Genes Dev. **11**, 1132–1139

10 Skoulakis, E. M. and Davis, R. L. (1998) 14-3-3 proteins in neuronal development and function. Mol. Neurobiol. **16**, 269–284

11 Morgan, A. and Burgoyne, D. (1992) Exo1 and Exo2 proteins stimulate calcium-dependent exocytosis in permeabilized adrenal chromaffin cells. Nature (London) **355**, 833–836

12 Broadie, K., Rushton, E., Skoulakis, E. M. and Davis, R. L. (1997) Leonardo, a Drosophila 14-3-3 protein involved in learning, regulates presynaptic function. Neuron **19**, 391–402

13 Fantl, W. J., Muslin, A. J., Kikuchi, A., Martin, J. A., McNicol, A. M., Gross, R. W. and Williams, L. T. (1994) Activation of Raf-1 by 14-3-3 proteins. Nature (London) **371**, 612–614

14 Reuther, G. W., Fu, H., Cripe, L. D., Collier, R. J. and Pendergast, A. M. (1994) Association of the protein kinases c-Bcr and Bcr-Abl with proteins of the 14-3-3 family. Science **266**, 129–133

15 Meller, N., Liu, Y. C., Collins, T. L., Bonnefoy-Berard, N., Baier, G., Isakov, N. and Altman, A. (1996) Direct interaction between protein kinase C theta (PKC theta) and 14-3-3 tau in T cells: 14-3-3 overexpression results in inhibition of PKC theta translocation and function. Mol. Cell. Biol. **16**, 5782–5791

16 Bonnefoy-Berard, N., Liu, Y.-C., von Villebrand, M., Sung, A., Elly, C., Mustelin, T., Yoshida, H., Ishizaka, K. and Altman, A. (1995) Inhibition of phosphatidylinositol 3-kinase activity by association with 14-3-3 proteins in T cells. Proc. Natl. Acad. Sci. U.S.A. **92**, 10142–10146

17 Morrison, D. (1994) 14-3-3 modulators of signalling proteins? Science **266**, 56–57

18 Rittinger, K., Budman, J., Xu, J., Volinia, S., Cantley, L. C., Smerdon, S. J., Gamblin, S. J. and Yaffe, M. B. (1999) Structural analysis of 14-3-3 polypeptide complexes identifies a dual role for the nuclear export signal of 14-3-3 in ligand binding. Mol. Cell **4**, 153–166

19 Chamberlain, L. H., Roth, D., Morgan, A. and Burgoyne, R. D. (1995) Distinct effects of a-SNAP, 14-3-3 proteins and calmodulin on priming and triggering of regulated exocytosis. J. Cell Biol. **130**, 1063–1070

20 Roth, D. and Burgoyne, R. D. (1995) Stimulation of catecholamine secretion from adrenal chromaffin cells by 14-3-3 proteins is due to reorganization of the cortical actin network. FEBS Lett. **374**, 77–81

21 Roth, D., Birkenfeld, J. and Betz, H. (1999) Dominant negative alleles of 14-3-3 proteins cause defects in actin organization and vesicle targeting in the yeast *Saccharomyces cerevisiae*. FEBS Lett. **460**, 411–416

22 Bamburg, J. R. (1999) Proteins of the ADF/cofilin family: Essential regulators of actin dynamics. Annu. Rev. Cell Dev. Biol. **15**, 185–230

23 Agnew, B. J., Minamide, L. S. and Bamburg, J. R. (1995) Reactivation of phosphorylated actin depolymerizing factor and identification of the regulatory site. J. Biol. Chem. **270**, 17582–17587

24 Meberg, P. J., Ono, S., Minamide, L. S., Takahashi, M. and Bamburg, J. R. (1998) Actin depolymerizing factor and cofilin phosphorylation dynamics: Response to signals that regulate neurite extension. Cell Motil. Cytoskeleton **39**, 172–190

25 Chan, A. Y., Bailly, M., Zebda, N., Segall, J. E. and Condeelis, J. S. (2000) Role of cofilin in epidermal growth factor-stimulated actin polymerization and lamellipod protrusion. J. Cell Biol. **148**, 531–542

26 Birkenfeld, J., Kartmann, B., Betz, H. and Roth, D. (2001) Cofilin activation during Ca^{2+}-triggered secretion from adrenal chromaffin cells. Biochem. Biophys. Res. Commun. **286**, 493–498

27 Arber, S., Barbayannis, F. A., Hanser, H., Schneider, C., Stanyon, C. A., Bernard, O. and Caroni, P. (1998) Regulation of actin dynamics through phosphorylation of cofilin by LIM-kinase. Nature (London) **393**, 805–809

28 Yang, N., Higuchi, O., Ohashi, K., Nagata, K., Wada, A., Kangawa, K., Nishida, E. and Mizuno, K. (1998) Cofilin phosphorylation by LIM-kinase 1 and its role in Rac-mediated actin reorganization. Nature (London) **393**, 809–812

29 Stanyon, C. A. and Bernard, O. (1998) LIM-kinase 1. Int. J. Biochem. Cell Biol. **31**, 389–394

30 Nunoue, K., Ohashi, K., Okano, I. and Mizuno, K. (1995) LIMK-1 and LIMK-2, two members of a LIM motif-containing protein kinase family. Oncogene **11**, 701–710

31 Toshima, J., Ohashi, K., Okano, I., Nunoue, K., Kishioka, M., Kuma, K., Miyata, T., Hirai, M., Baba, T. and Mizuno, K. (1995) Identification and characterization of a novel protein kinase, TESK1, specifically expressed in testicular germ cells. J. Biol. Chem. **270**, 31331–31337

32 Toshima, J., Toshima, J. Y., Amano, T., Yang, N., Narumiya, S. and Mizuno, K. (2001) Cofilin phosphorylation by protein kinase testicular protein kinase 1 and its role in integrin-mediated actin reorganization and focal adhesion formation. Mol. Biol. Cell **12**, 1131–1145

33 Ohashi, K., Nagata, K., Maekawa, M., Ishizaki, T., Narumiya, S. and Mizuno, K. (2000) Rho-associated kinase ROCK activates LIM-kinase 1 by phosphorylation at threonine 508 within the activation loop. J. Biol. Chem. **275**, 3577–3582

34 Edwards, D. C., Sanders, L. C., Bokoch, G. M. and Gill, G. N. (1999) Activation of LIM-kinase by Pak1 couples Rac/Cdc42 GTPase signalling to actin cytoskeletal dynamics. Nat. Cell. Biol. **1**, 253–258

35 Sumi, T., Matsumoto, K., Shibuya, A. and Nakamura, T. (2001) Activation of LIM-kinases by myotonic dystrophy kinase-related Cdc42-binding kinase α. J. Biol. Chem. **276**, 23092–23096

35a Bernard, O., Ganiatsas, S., Kannourakis, G. and Dringen, R. (1994) Kiz-1, a protein with LIM zinc fingers and kinase domains, is expressed mainly in neurons. Cell Growth Differ. **5**, 1159–1171
36 Birkenfeld, J., Betz, H. and Roth, D. (2001) Inhibition of neurite extension by overexpression of individual domains of LIM kinase 1. J. Neurochem. **78**, 924–927
36a Watanabe, M., Isobe, T., Ichimura, T., Kuwano, R., Takahashi, Y., Kondo, H. and Inoue, Y. (1994) Molecular cloning of cDNAs for the zeta and theta subtypes of 14-3-3 protein and differential distribution of their mRNAs in the brain. Mol. Brain Res. **25**, 113–121
37 Harlow, E. and Lane, D. (1988) Antibodies: A Laboratory Manual, Cold Spring Harbour Laboratory Press, Cold Spring Harbor, NY
38 Edwards, D. C. and Gill, G. N. (1999) Structural features of Lim kinase that control effects on the actin cytoskeleton. J. Biol. Chem. **274**, 11352–11361
39 Hashiguchi, M., Sobue, K. and Paudel, H. K. (2000) 14-3-3ζ is an effector of tau protein phosphorylation. J. Biol. Chem. **275**, 25247–25254
40 Liao, J. and Omary, M. B. (1996) 14-3-3 proteins associate with phosphorylated simple epithelial keratins during cell cycle progression and act as a solubility factor. J. Cell Biol. **133**, 345–357
41 Tzivion, G., Luo, Z. J. and Avruch, J. (2000) Calyculin A-induced vimentin phosphorylation sequesters 14-3-3 and displaces other 14-3-3 partners in vivo. J. Biol. Chem. **275**, 29772–29778
42 Toshima, J. Y., Toshima, J., Watanabe, T. and Mizuno, K. (2001) Binding of 14-3-3 beta regulates the kinase activity and subcellular localization of testicular protein kinase 1. J Biol Chem. **276**, 43471–43481
43 Vincenz, C. and Dixit, V. M. (1996) 14-3-3 proteins associate with A20 in an isoform-specific manner and function both as chaperone and adapter molecules. J. Biol. Chem. **271**, 20029–20034
44 Zhai, J., Lin, H., Shamim, M., Schlaepfer, W. W. and Canete-Soler, R. (2001) Identification of a novel interaction of 14-3-3 with p190RhoGEF. J. Biol. Chem. **276**, 41318–41324

Received 22 July 2002; accepted 26 September 2002
Published as BJ Immediate Publication 26 September 2002, DOI 10.1042/BJ20021152